SINGLE PARTICLE FLUORESCENCE BURST ANALYSIS OF MEMBRANE FISSION

A Thesis

by

ARIELLE LEA BROOKS

Submitted to the Office of Graduate and Professional Studies of
Texas A&M University
in partial fulfillment of the requirements for the degree of

MASTER OF SCIENCE

Chair of Committee,	Hays S. Rye
Committee Members,	James Hu
	Mark Harlow
	Jean-Philippe Pellois
Head of Department,	Gregory D. Reinhart

May 2015

Major Subject: Biochemistry

ABSTRACT

The ability to catalyze the fission step of endocytosis is critical to many biological processes including cell communication and synaptic transmission. This activity must be tightly regulated for cellular homeostasis. Limitations of current approaches used for the study of this process, in conjunction with a historical focus on neuronal systems that may not generalize to somatic cells, have left the field torn between several conflicting models. Functional redundancy of several key players complicate interpretation of *in vivo* studies, stressing the need for a sensitive *in vitro* approach capable of revealing attenuated activity of tightly regulated machinery. In this document, we introduce Burst Analysis Spectroscopy (BAS) as a simple reagent sparing approach for the investigation of vesicle membrane fission. Using BAS, we accurately map liposome distributions across several orders of magnitude and observe subtle shifts in liposome population as functions of time, temperature, and protein concentration using the fission potent ENTH domain of the protein epsin. We proceed to further uncover an unrecognized fission activity of full-length epsin, consistent with a mechanism in which membrane fission proceeds as a consequence of amphipathic helix insertion into the lipid bilayer.

ACKNOWLEDGEMENTS

I would like to thank my committee chair, Dr. Rye, and our senior lab researcher, Dr. Carr, for their instrumental guidance and support throughout the course of this research. I would also like to thank my committee members, Dr. Harlow, Dr. Hu, and Dr. Pellois for all of their input and support throughout my career at Texas A&M. Finally, I want to thank my family and friends for all their love and support when I needed it the most.

TABLE OF CONTENTS

LIST OF FIGURES

CHAPTER I

INTRODUCTION AND LITERATURE REVIEW*

Dynamin as the core fission machinery

The ability of cells to internalize and transport molecular cargo is critical to vital cellular processes including cell communication and synaptic transmission. In order to impart specificity to the timing and integrity of fission, proteins specialized to catalyze fission and fusion have evolved. In the fission step of endocytosis, the membranous bud pinches off from the donor membrane forming a complete and discrete vesicle. To date, much of our understanding of membrane fission has focused on one of the first proteins implicated in endocytosis: dynamin.

In the 25 years since the implication of the protein dynamin in endocytosis, extensive research has focused on illuminating its role in this integral life process. Dynamin was initially found as a GTP-dependent regulator of microtubule interactions in calf brain [1]. As a consequence of this this historical precedent, much of our current understanding of the role of dynamin in membrane fission is based on studies of neuronal dynamin. Despite years of research on this topic, the detailed molecular mechanism by which dynamin catalyzes fission remains a topic of debate.

Dynamin is believed to function by using the energy from GTP hydrolysis to bring donor membranes into very close proximity, enabling the formation of fission

---

*Parts of this thesis are reproduced with permission, with changes, from Single Particle Fluorescenec Burst Analysis of Espin Induced Membrane Fission by Brooks, et al. *PLoS ONE* **10**, e0119563 (2015).

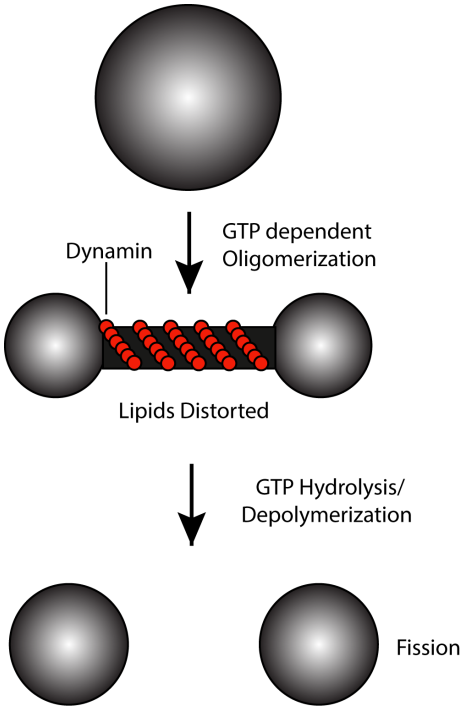

Figure 1. Canonical model for membrane fission. Dynamin oligomerizes into long spirals along lipid template upon GTP addition. Cooperative GTP hydrolysis and subsequent depolymerization results in membrane fission. Adapted from [2].

intermediates (Figure 1)[3]. An important element in this process is the ability of dynamin to oligomerize along lipid membranes to generate tube-like extensions called tubules [3].

This ability can be visualized *in vitro* by negative staining electron microscopy, where dynamin is observed distorting acidic liposomes into long tubules in the presence of non-hydrolyzable GTP analogs [3]. For years, researchers focused on the formation of these intermediates with the assumption that fission cannot proceed in their absence. However, advances in techniques utilized to study this process revealed that these long tubules are not integral intermediates, but rather a dead end for the fission process [4].

Instead, GTP hydrolysis is required for the dynamin depolymerization required for the formation of extremely short, transient tubules that precede fission [5]. Despite advances in technology, the mechanism by which dynamin facilitates the formation of fission intermediates remains a topic of debate. Moreover, recent findings call the dogmatic model of dynamin as the core fission machinery into question.

Part of the difficulty in deciphering the minimal machinery for fission may stem from the historical precedent of neuronal dynamin. Since its discovery, additional dynamin isoforms have been identified that are preferentially expressed in non-neuronal tissues [6]. Notably, these isoforms do not behave like neuronal dynamin (dyn1) in fission reactions [6]. In fact, the ubiquitously expressed dynamin-2 (dyn2) has dramatically lower fission activity than neuronal dynamin. This suggests that clues for a general mechanism of fission may be found through studies of non-neuronal proteins. Lending support to this idea is the fact that several fission events occur in the cell that do not require a dynamin or dynamin-like protein, as is the case for ER-to-Golgi trafficking, which uses COPI and COPII for vesicle formation [7].

Current models for fission

Several models have been proposed for the mechanism of vesicle fission. The canonical model for fission casts dynamin as a molecular "pinchase". According to this model, dynamin assembles into long spiral oligomers in the presence of lipid substrate generating long tube-like extensions called tubules [8] (Figure 1). Upon GTP hydrolysis, a conformational change is induced resulting in a significant decrease in the diameter of

the underlying lipid tubule. This is thought to bring membranes in close enough proximity to facilitate the formation of a hemifusion (or in this case, hemifission) intermediate [3]. However, theoretical calculations propose a minimum radius of 3 nm for spontaneous fusion [9], while electron cryo-microscopy (Cryo-EM) studies have measured the smallest dynamin-induced constriction at 4.5 nm [10]. According to this canonical model, dynamin is the core fission machinery. Binding partners including the lipid binding proteins amphiphysin and epsin act as accessory proteins, playing roles either in recruitment or the initial generation of curvature and pit formation required for dynamin binding [11;12].

An alternative model focuses on the role of amphipathic helix insertion in fission catalysis. Amphipathic helices such as those found on the dynamin binding partner epsin have been demonstrated to insert into a single leaflet of a membrane bilayer in a process known as hydrophobic insertion. Shallow asymmetrical insertion of these helices is traditionally believed to result in the expansion of the donor leaflet, resulting in curvature generation [13]. In stark opposition to the canonical model, the hydrophobic insertion model for fission asserts that vesicle fission proceeds as a result of membrane instability induced by the insertion of these helices into one leaflet of a donor membrane [14].

This model is explained by the consideration of an obligate funnel-like fission intermediate illustrated in Figure 2. Researchers concluded using computational analyses that shallow hydrophobic insertions into the bilayer are capable of "[expanding] the head group region with respect to the bilayer midplane", culminating in a

destabilization of the neck and subsequent fission [14]. Consistent with this model, the amphipathic helix-containing protein Sar1 is capable of membrane fission catalysis [7]. This model casts dynamin as a regulatory protein, possibly required for curvature generation.

Recently, a middle ground has emerged in which these proteins are believed to function synergistically, such that amphiphysin dramatically enhances inefficient dynamin fission activity [15]. According to this synergistic model, dynamin still serves as the core mechanical pinchase required for fission while accessory proteins such as amphiphysin and epsin induce curvature and enhance the intrinsic fission activity of dynamin. Instead of serving as the core machinery for fission, this model asserts that amphipathic helix insertion is important for spatio-temporal regulation for the prevention of aberrant fission (Reviewed in [16]). Interestingly, all of these models are consistent with the phenotypes observed by knockdowns *in vivo* [17]. As functional redundancy and alternative pathways obscure clear phenotypes *in vivo*, we believe that a simple *in vitro* assay for fission is required to ascribe clear roles to the proteins involved in the fission reaction.

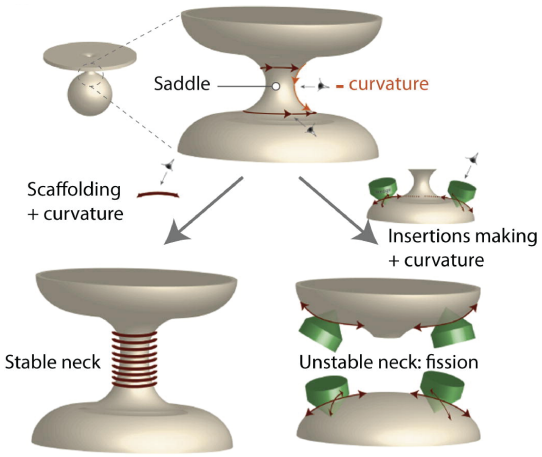

Figure 2. Hydrophobic insertion favors membrane fission. According to the predictions of Boucrot et al., scaffolding proteins such as amphiphysins (red) stabilize the saddle-shaped neck between two connected membranes, while hydrophobic insertions (green wedges) destabilize the neck, facilitating fission. Figure from [14].

Limitations of current methods

While much progress has been made in the identification and mechanism of membrane fusion proteins[18; 19], the mechanism of membrane fission remains a topic of heated debate. Current approaches often rely on ensemble measurements that are prone to artifacts due to sample handling. For example, negative staining electron microscopy is often used as a standard for the assessment of liposome fission. In this technique, researchers analyze the size and shape of starting liposomes and compare the products following protein addition. However, not only is interpretation of these images complicated by the presence of staining artifacts, but results are confounded by fission induced by the mechanical stress of sample preparation, as well [3].

Membrane tethers pulled from giant unilamellar vesicles have been used to address some of the limitations of ensemble methods. However, these assays are unable to provide quantitative measurements of fission efficiency, are time intensive, require highly specialized equipment and highly skilled hands, and do not provide many events to draw statistically robust conclusions [20]. Supported bilayers with excess membrane reservoir (SUPER) templates have been introduced as an alternative approach to membrane tethers [21]. These SUPER templates allegedly serve as an easy fluorescence based technique that facilitates quantitative, real-time analysis of membrane fission events. However, this technique relies on the quantification of small weak fluorescent vesicles in the presence of a highly fluorescent giant unilamelar vesicle (GUV). As a consequence, they are limited in their ability to detect rare fission events that may be characteristic of the attenuated fission activity of a tightly regulated machine in the

absence of effectors. Furthermore, SUPER templates are highly prone to artifacts from mechanical shearing [22]. Thus, inefficient fission resulting from a tightly regulated machine may be perceived as an artifact as it is in the noise of such insensitive techniques.

In a recent paper, a novel ensemble sedimentation-based fission assay was used to demonstrate the potent fission activity of the ENTH domain of the protein epsin [14]. Unfortunately, this assay can only identify dramatic shifts in liposome populations, is protein expensive, and cannot be used to provide valuable kinetic information. Membrane fission is a complex and dynamic process that, due to its critical importance in biological function, is likely to require a coordinated system of tightly regulated and sometimes redundant activity. Consequently, an extremely sensitive technique capable of detecting subtle changes in vesicle populations as a function of time and protein is required. In order to establish such a technique, we chose to focus on the ENTH domain of epsin with the intention of recapitulating the authors' findings with the refined details required for this intricate process.

Epsin as a fission catalyst

Epsin is a 94 kDa protein identified in screens for binding partners of α-adaptin and Eps15, both clathrin coat associated proteins involved in clathrin-mediated endocytosis in neurons [23;12]. Epsin is generally believed to function in cargo selection and bud site nucleation through direct interactions with Eps15, the clathrin adaptor protein, AP-2, endocytic cargo and with clathrin itself (reviewed in [24]). At the amino terminus of epsin

is the highly conserved, ~140 amino-acid ENTH domain shared with other endocytic proteins, including AP180/CALM [25]. This domain contains an N-terminal amphipathic helix (the H_0 helix), which is known to insert into the outer-leaflet of membranes in a PtdIns(4,5)P_2-dependent fashion [26]. Membrane insertion of the H_0 helix is thought to facilitate membrane curvature and tubulation prior to fission.

Recently, it was suggested that insertion of the ENTH H_0 helix into a lipid bilayer could directly facilitate fission [14]. This work reported potent fission activity when liposomes were mixed with the isolated ENTH domain, though full-length epsin did not appear to possess fission activity. However, the conclusion of these results has been called into question [15]. Concerns exist that the observed ENTH-mediated fission activity are artifacts of high concentrations of a non-native protein domain interacting non-specifically with liposomes to form micelles. The controversy surrounding this recent dogma-shattering finding exemplifies the need for a simple, protein inexpensive method that allows for quantitative analysis of the fission process.

Burst Analysis Spectroscopy: A novel approach for the study of vesicle fission

Unlike current methods for the study of fission, Burst Analysis Spectroscopy (BAS) is a reagent sparing single particle technique that is well suited to the investigation of vesicle fission. Unlike sedimentation, BAS permits the mapping of the full distribution of liposomes in a sample. Unlike methods such as fluorescence correlation spectroscopy (FCS), BAS does not rely on diffusion and thus is not limited to a narrow range of particle brightness distribution. BAS differs from diffusion-limited

approaches such as FCS in the utilization of a moving stage. For BAS analysis, a sample scan rate is chosen that greatly exceeds the rate of transit due to free diffusion of a particle. The BAS analysis is a recursive analysis in which the largest bursts are attributed to the brightest particles passing through the center of the excitation beam. The analysis corrects for the position of a fluorescent particle within the excitation beam as described in [27]. Consequently, it is possible to track both the disappearance of large material and the concomitant appearance of intermediate and small material across several orders of magnitude. BAS facilitates the mapping of subtle shifts in population, allowing us to observe changes as a function of time and protein concentration. This can prove invaluable in the identification of key players of the fission reaction, permitting the visualization of attenuated fission activity in the absence of regulatory factors.

Goal of thesis research

The goal of this thesis is to introduce burst analysis spectroscopy as a novel, single particle assay for the investigation of membrane fission. Using BAS, we were able to accurately map liposome distributions across several orders of magnitude without many of the sample-handling artifacts that confound traditional techniques.

CHAPTER II

ESTABLISHING BAS AS SINGLE PARTICLE ASSAY FOR VESICLE FISSION

The ability to distinguish between several proposed models for fission is hindered in part by the current techniques used to investigate this process. We have developed a single-particle, free-solution membrane fission assay based on BAS that avoids the artifacts of surface-tethered fusion assays and provides a large number of events for statistically robust conclusions. To establish this assay, we have analyzed changes in liposome populations as a function of time, temperature, and protein concentration using the fission potent ENTH domain from the protein Epsin. This is the first fission assay that facilitates the analysis of kinetics on a minute timescale. Using this kinetic information, we ultimately hope to further probe the mechanisms of these reactions. In this chapter we aim to introduce BAS as a rapid and reagent sparing method to screen for the function of proteins involved in the fission process.

Methods

Protein expression and purification. The epsin ENTH domain (residues 1-164) from *Rattus norvegicus* was cloned into the NarI and SacI sites of the pPROEX HTb vector. For purification, His6-ENTH (hereafter ENTH) transformed BL21 cells were used to inoculate 2 L Terrific Broth cultures at a 1:500 dilution. Cells were grown at 37°C, to A600 = 0.45. Cultures were incubated at 18 °C and induced at A600 = 0.6 with 400 μM IPTG. Cells were harvested by sedimentation after incubation at 18 °C for 16

hr. Cell pellets were lysed in Ni-NTA Buffer A (20 mM Tris pH 8, 500 mM NaCl, 20 mM imidazole, 5 mM β-mercaptoethanol) using a pre-chilled microfluidizer (Watts Fluidair, Inc., Kittery, ME). Lysates were clarified at 4 °C, by centrifugation for 45 min at 100,000 xg. The supernatant fraction was loaded over a Ni-NTA column (Qiagen) equilibrated in Ni-NTA Buffer A, and eluted with 20% Ni-NTA Buffer B (20mM Tris pH 8, 500 mM NaCl, 500 mM Imidazole, 5 mM β-mercaptoethanol). The His6 tag was cleaved with His6-tEV protease during dialysis against Ni-NTA Buffer A at 4 °C. The His6 tag and His6-tEV were removed using the Ni-NTA column equilibrated in Ni-NTA Buffer A. ENTH-containing fractions were concentrated to 500 µL and diluted into Source S Buffer A (20 mM Tris pH 7.4, 2 mM DTT). Further purification of ENTH was achieved using a linear gradient from 0-100% Source S Buffer B (20 mM Tris pH 7.4, 2 mM NaCl, 2 mM DTT) over a Source S column. Pure ENTH was buffer exchanged to 20 mM Tris pH 7.4, 150 mM KCl, 2 mM DTT and snap frozen in liquid nitrogen for storage at -80 °C. Full-length rat epsin was cloned into the SgfI and NotI sites of the PEX-N-His6-GST vector. His6-GST-epsin (hereafter epsin) transformed BL21 DE3 cells were used to inoculate 2L LB cultures at a 1:500 dilution. Cells were grown at 37 °C, induced at A600 = 0.6 with 400 uM IPTG and harvested after 4 hrs. Full-length rat epsin was cloned into the pEX-N-His6-GST vector (Origine) for expression in E. coli BL21[DE3] and purification by the same affinity chromatography and proteolytic cleavage protocol, followed by high-resolution ion exchange chromatography on a Mono Q column to separate full-length epsin from degradation products.

Liposome Peparation. Liposomes were prepared as previously described, with minor modifications [14]. Briefly, brain lipid extracts from Avanti (cat. 131101P) and Sigma (cat. B-1502) were mixed 1:1, with 5% PtdIns(4,5)P_2 (Avanti, cat. 840046C) and 0.03% acyl-chain, Ω−carbon labeled TopFluor-PtdEth (Avanti, cat. 810282C). Lipids dried under a stream of argon and vacuum dessicated to remove residual solvents were suspended, with freezing and thawing, to 1 mg/ml in liposome buffer (20 mM HEPES pH 7.4, 200 mM NaCl) and extruded through polycarbonate filters with the indicated diameters with 11 passes in a mini extruder (Avanti), followed by 10 passes through a high-pressure manifold extruder (Northern Lipids), and used within 6 hr. Liposomes used at later times no longer respond to addition of ENTH domain or epsin, presumably due to loss of liposome binding upon PtdIns(4,5)P_2 hydrolysis. Liposome integrity was verified in a separate experiment (not shown), by including a luminal dye, Alexa647 carboxylate, during extrusion and observing coincidence of TopFluor-PE and Alexa647 bursts by BAS.

Liposome fission assay by BAS. Liposomes diluted to 0.01 mg/mL in liposome buffer were mixed with ENTH domain, or full-length epsin, at the concentrations indicated, and 10 µL of the each sample was spotted onto a BSA-blocked glass coverslip held in a custom cassette. The coverslip cassette was clamped to a high-precision, computer controlled, 2-axis translation stage connected to a customized microscope system, and data were collected as previously described ([27];[28]). Efficient fission of large (~ 200 nm) liposomes into small (20-30 nm) liposomes should result in a large (100 to 200-fold) increase in object concentration, read out as fluorescent bursts with amplitudes

proportional to the object sizes. From a starting sample of 50-100 pM large liposomes, this increase in object number will violate the single-particle concentration limit (< 500 pM) required for BAS. Additionally, due to limited knowledge of the instrument point spread function, an individual BAS measurement can only quantitatively probe an approximately 100-fold range in object intensity for a single, uniformly labeled species [27]. The fission of large liposomes into much smaller ones leads to a highly inverted population dominated by smaller particles. In this case, the resolving power of BAS deteriorates for the low intensity events, due to the high species concentrations that no longer permit single particle detection. Therefore, to accurately examine liposome populations produced during fission, we developed an enhanced measurement protocol that permits BAS histograms to be constructed over an arbitrarily large range of object sizes. In brief, standard BAS data are collected on a series of systematic dilutions of each reaction sample, followed by analytical reconstruction of the overall population distribution through simultaneous fitting of the object cumulative distributions across the dilution series. Our standard BAS analysis fitting routines [27] have been modified to accommodate this expanded data analysis strategy. The fitting and programmatic details will be published elsewhere.

Heat maps. In order to better visualize the information obscured by BAS histograms, we provide an alternative "heat map" figure. Plots representing the spread of liposome products as a function of time or concentration are shown as a "heat maps": a stack of rows, one experiment per row, with increasing brightness corresponding to an increased fractional intensity of each bin (group of burst events of a

given size). To convert the number of burst events in each bin to fractional intensity, we normalized the object intensities as follows:

$$\frac{I_i C_i}{\sum_{n=i}^{i} I_n C_n} \quad (1)$$

where I_i is the intensity of each bin, C_i is the concentration of objects in each bin, and the denominator represents the total fluorescence of all bins (the sum of intensity in a row) for a given sample.

Results and discussion

BAS is sensitive to changes in liposome size and concentration. In order to calibrate our BAS measurements of membrane fission, we first examined a series of liposome standards created with different diameters. Liposomes were extruded to 200 nm, 100 nm, and 50 nm and then examined by BAS. Single-particle burst data for these samples display the expected dependence of burst size on liposome size (Figure 3a). The fluorescence intensity of these membrane labeled liposomes is expected to be proportional to their surface area; thus, the mean intensity of the 200 nm versus 100 nm, as well as the 100 nm versus the 50 nm liposomes should differ by ~ 4-fold and the 200 nm and 50 nm should differ by ~ 16-fold. As shown in Figure 3b, the BAS histograms of each liposome sample display distributions with mean intensity differences consistent with the expected values. Additionally, the dispersion in liposome sizes measured by

BAS is consistent with the expected variation for liposomes created by extrusion, specified as ± 25% CV (coefficient of variation; Northern Lipids specifications). As shown in Figure 3b, the observed size variation in liposomes appears to be between 35-50 % CV, based on Monte Carlo simulations of particle distributions in which the particle brightness is assumed to be proportional to surface area. While the observed liposome variation is somewhat larger than expected, several factors likely broaden the observed intensity distribution, including a small fraction of multi-lamellar objects (30) and the discreet distribution of dye molecules between objects of the same absolute size. As a complementary measurement, we examined each liposome sample by FCS (Figure 3c). FCS provides information on hydrodynamic radius based on measurement of the average diffusion time of fluorescent objects as they diffuse in and out of the excitation beam. However, diffusion time increases linearly with particle radius and so is not as sensitive a measure of liposome size as fluorescence intensity, which increases with the square of the radius. Additionally, FCS is dependent on particle surface hydrophobicity so that the hydrodynamic radius can be converted to an effective size only with knowledge of this surface-solvent interaction. Therefore, we use FCS here primarily as an indicator of a difference in average population hydrodynamic radius. Consistent with the BAS measurements, the mean diffusion time for each liposome sample decreases as the extrusion filter pore diameter decreases (Figure 3c).

Membrane fission activity of the Epsin ENTH domain. We next examined the ability of BAS to detect products of ENTH domain-mediated fission. Samples of large

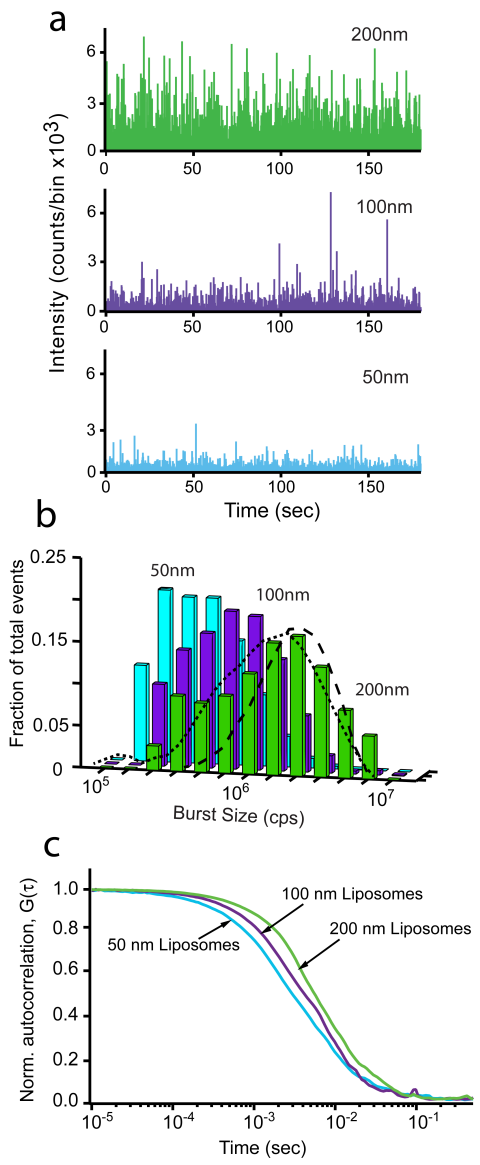

Figure 3. BAS assay distinguishes liposomes of different sizes. The size distribution of 200 nm, 100 nm and 50 nm fluorescent liposomes was examined by FCS and BAS. (a) Fluorescent burst data of TopFluor-labeled Folch liposomes extruded to 200 nm (green), 100 nm (purple) and 50 nm (cyan). (b) BAS histograms generated from the burst data in (a). Fraction of total events is the concentration of each bin divided by the total concentration, for each sample. Dashed lines show theoretical diameter distributions (35% CV, dash; 50% CV, dot) derived from Monte Carlo simulated intensity data in which fluorescence brightness was set proportional to particle surface area. The resulting simulated intensity distributions were analyzed with BAS analysis code. (c) FCS profiles of 200 nm, 100 nm, and 50 nm liposomes. The data shown is representative of two experimental replicates.

liposomes (either 400 nm or 200 nm) were mixed with purified ENTH domain and then examined by BAS after 40 min incubation at 37 °C. We anticipated fission to be detectable as a shift from a small number of large fluorescence bursts to a larger number (high concentration) of much smaller bursts. As shown in Figure 4 a-d, the expected changes are observed upon addition of the ENTH domain to either 400 nm, or 200 nm liposomes. Importantly, the total fluorescence intensity of the sample before and after ENTH addition changed by no more 10-15% (data not shown), demonstrating that the observed disappearance of the large bursts was not caused by a loss of the starting liposomes, but rather by their conversion into a high concentration of smaller objects.

The extent of fission of the 200 nm liposomes was quantified by BAS analysis of the raw burst data. The resulting BAS histograms display a dramatic shift from a low concentration of large liposomes to an increased concentration of small ones (Figure 4e). The smallest products of the fission process (Figure 4e, inset) increase by over 100-fold relative to the staring concentration of 200 nm liposomes, consistent with the number of small liposomes expected from efficient fission of the starting 200 nm liposomes into ~ 20 nm products. A similar scaling argument predicts that the mean burst size of a 20 nm product liposome should be ~ 100-fold smaller than the mean burst size of a starting 200 nm liposome, assuming that segregation of the fluorescent label is not biased by the process of fission. As shown in Figure 4e, the relative difference in mean burst size for the staring and product liposomes is consistent with the product liposomes being ~ 20 nm in size. The product liposome distribution is most consistent with an approximately

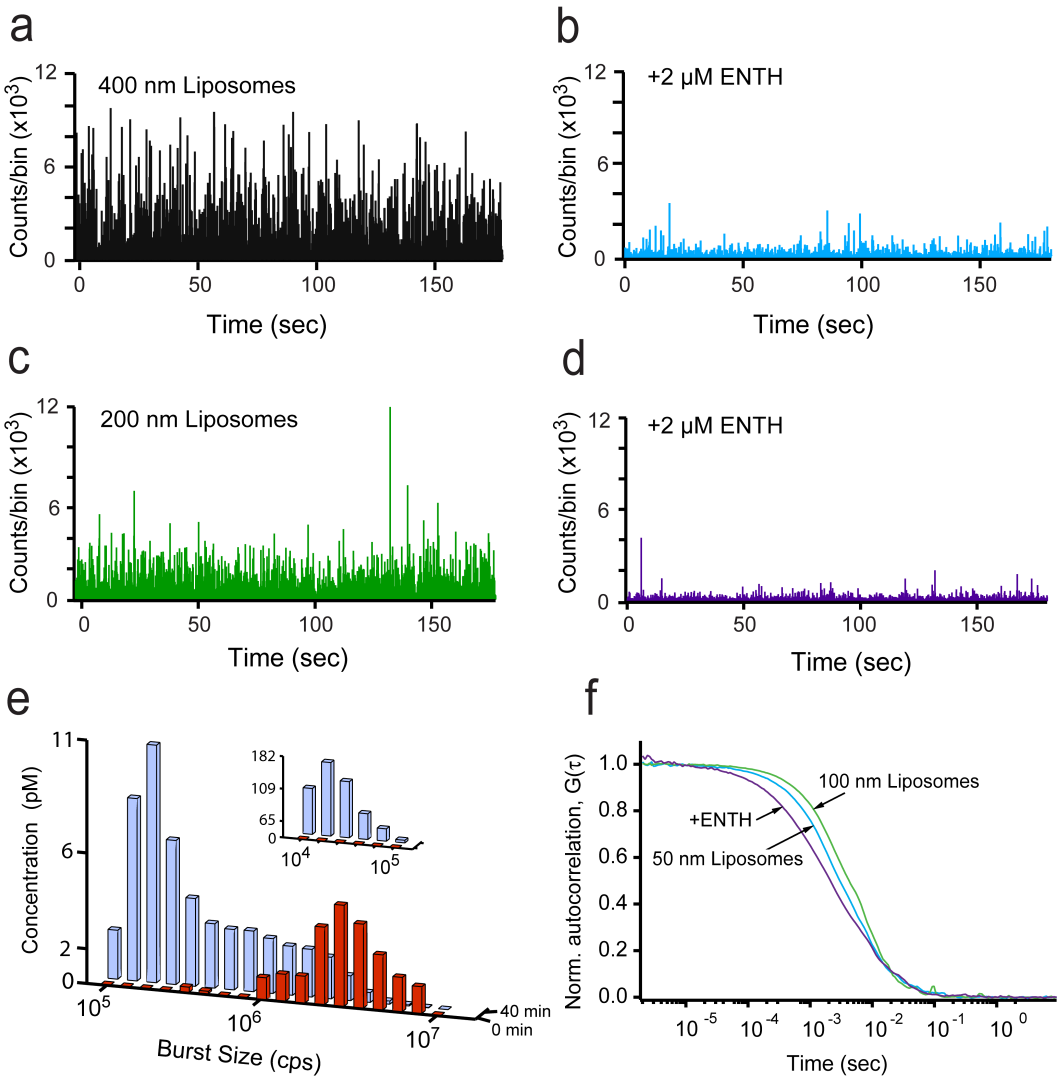

Figure 4. BAS analysis of liposomes vesiculated by the ENTH domain of epsin. Fluorescent burst data for 400 nm-diameter, TopFluor-labeled, (5%) PtdInsP(4,5)P2 Folch liposomes 380 incubated at 37 °C for 40 min before (a) and after addition of 2 μM ENTH (b). Fluorescent burst data for Single particle analysis of membrane fission 17200 nm-diameter liposomes incubated at 37 °C for 40 min before (c) and after addition of 2 μM ENTH (d). (e) BAS histograms generated from starting 200 nm liposomes before (red) and after addition of ENTH (blue; insets indicate resolution of small particles in a 10-fold dilution of the same reaction). (f) FCS profiles of liposomes extruded to 100 nm (green), 50 nm (cyan) and the end products (purple) of the fission reaction of 200 nm liposomes from (d). The data shown is representative of three experimental replicates. The data shown is representative of 3 experimental replicates.

30% CV (20 nm ± 6 nm), based on comparison of the intensity variation in the smallest product liposomes with simulated particle populations created at different size variations (10-50% CV; see Figure 3b for an example). Examination of samples by FCS is also consistent with efficient membrane fission. Liposomes mixed with the ENTH domain show a dramatic shift in average diffusion time to values substantially less than that observed for 50 nm liposomes (Figure 4f). Taken together, these observations are consistent with the generation of ~ 20 nm vesicles by the ENTH domain, as previously observed by electron microscopy [14].

The ENTH domain acts on the timescale of minutes. The sensitivity of BAS permits changes in the liposome population as a function of time to be mapped with far greater accuracy than achieved previously. After 20 min at 23 °C, a significant shift in the vesicle population size distribution is observed. However, some large vesicles remain (Figure 5a, b). By 60 min, the largest vesicles are observed rarely, and the disappearance of large vesicles is concurrent with the appearance of smaller ones over the full 100-minute time course. The fission activity of the ENTH domain is enhanced at 37 °C (Figures 5c, d), with the largest vesicles observed rarely at 20 min. At 37 °C, the reaction appears to be complete by 80 min, consistent with the 100 min time point at 23 °C.

In order to more fully illustrate the changes in liposome populations as a function of time, we normalized the fractional intensity of each BAS intensity bin and re-plotted the data as a heat map (see methods; Figure 5c). While the large starting liposomes at time zero form a bright peak on the right end of the plot, at later time points, the

fractional fluorescence is distributed between small and medium products. These eventually populate a bright peak of small liposomes at the top (left), plus a lower concentration of broadly distributed medium-sized liposomes. Whether these intermediate-sized liposomes are static end products or the result of additional liposome dynamics is unknown, but they persist regardless of protein concentration or time. Notably, the rate at which the largest liposome population disappears does not appear to be detectably different at 23 °C and 37 °C. This observation is likely due to the small fractional change in intensity that occurs when 20 nm liposomes split from the much larger 200 nm liposome objects. The resulting 1-2% change in fluorescence intensity is not detectable in this assay, given the difference in the rate of fission at the two temperatures. However, the smallest products reach their maximum concentration at ~ 30 min at 37 °C and ~ 60 min at 23 °C, indicating a ~ 2-fold increased rate at 37 °C.

Fission activity of the ENTH domain is dose-dependent. Next, we looked for a dose-dependent change in fission activity of the ENTH domain. In order to maximize the sensitivity of observable changes in the liposome size-distribution, we chose an early time point in the fission reaction (20 min at 37 °C) and focused on the disappearance of large liposomes and appearance of intermediate-sized products (without the dilutions required to resolve small products). Using this approach, we were able to measure fission activity at concentrations as low as 500 nM ENTH domain (Figures 6a,b). At this early time point, the fission activity increases as a function of protein concentration up to 10 mM (Figure 6a, b).

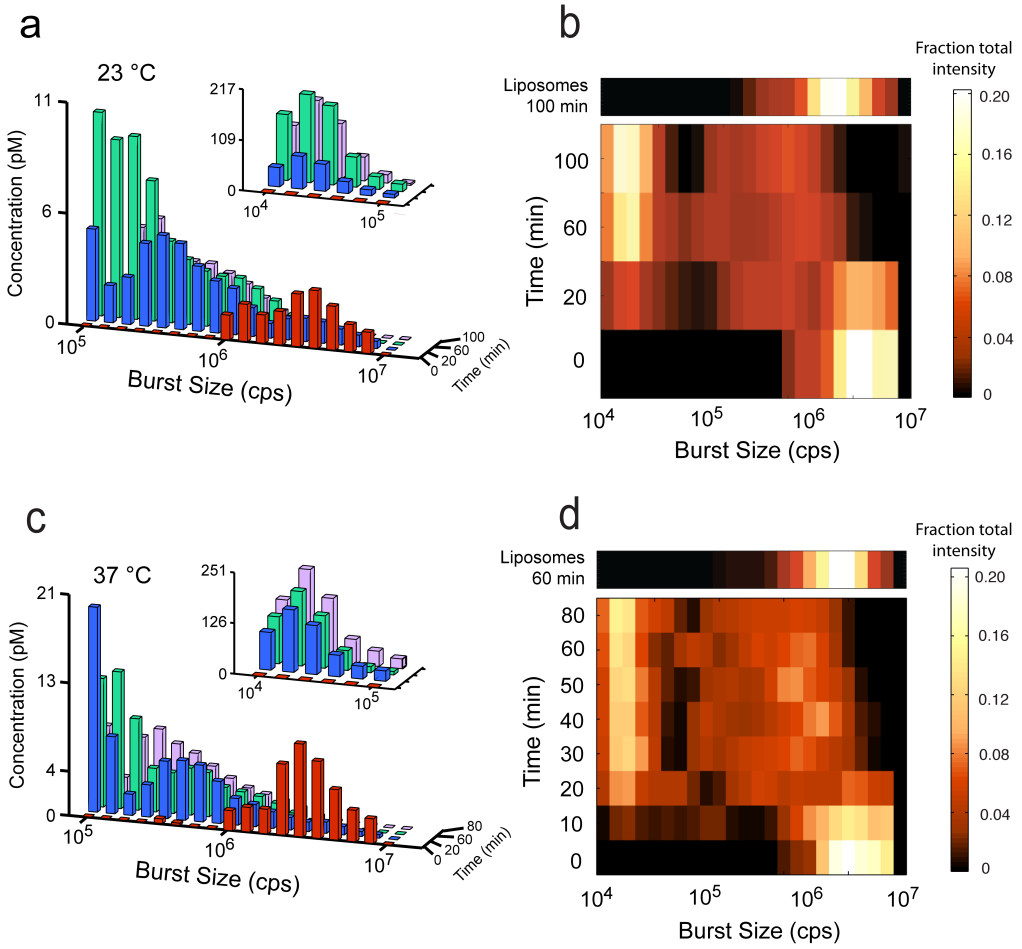

Figure 5. Kinetics of liposome fission are temperature dependent. (a) Histograms of BAS analyzed 200 nm-diameter, TopFluor-labeled, (5%) PtdInsP(4,5)P2 Folch liposomes (red) and products of ENTH incubation at 23 °C for 20 (blue), 60 (green), and 100 min (purple) after addition of 2 μM ENTH. At each time point, an aliquot was removed and placed on ice, and measurements were started within 1-2 min. Inset indicates resolution of small particles in a 10-fold dilution of each reaction. (b) Heat map representation of the fractional intensity for each reaction shown in (a). (c) BAS histograms generated from starting liposomes (red) and products of ENTH incubation at 37 °C for 20 (blue), 60 (green), and 80 min (purple) after addition of 2 μM ENTH. (d) Heat-map representation of the fractional intensity for each reaction shown in (c). Additional time points are shown for increased resolution. The effect of incubating liposomes in the absence of the ENTH domain for 60 min at 37 °C or 100 min at 23 °C is shown as an additional row, above the respective heat maps. The data shown for the experiments conducted at 23 °C is representative of four experimental replicates. The data shown for experiments conducted at 37° C is representative of three experimental replicates.

Fission activity of full-length epsin. While the results of these and previous studies [14] indicate potent membrane fission activity for the epsin ENTH domain, it remained possible that the activity we observed is an artifact of the truncation and not a function of the full-length epsin protein. We reasoned that if epsin has latent membrane fission activity, then we might uncover that activity using the high sensitivity of BAS and conditions that maximize fission activity for the ENTH domain. Using this approach, we observed dose-dependent liposome fission activity at epsin concentrations as low as 1 μM, albeit with significantly slower rates than observed for the ENTH domain (Figures 7a, b). To compensate for the slower rates, dose-dependence of epsin activity was measured at a 40 min time point and compared to the earlier 20 min time point used for the ENTH domain (Figure 6).

Despite the kinetic differences, the distribution of liposome products is remarkably similar and converges to the same size end products after a 90 min incubation. These results suggest that both the ENTH domain and the full-length epsin protein employ the same membrane-fission mechanism (Figure 7c). Using BAS, we observed time-resolved liposome membrane fission in free solution, induced by the potent epsin ENTH domain. These results agree with those of a previous study that demonstrated that the ENTH domain of Epsin is necessary and sufficient for endocytic vesicle membrane fission using a novel sedimentation assay and *in vivo* analysis [14]. Recently, concerns were raised regarding the physiological significance of the fission activity observed in that study, specifically citing the small size of the liposomes (200

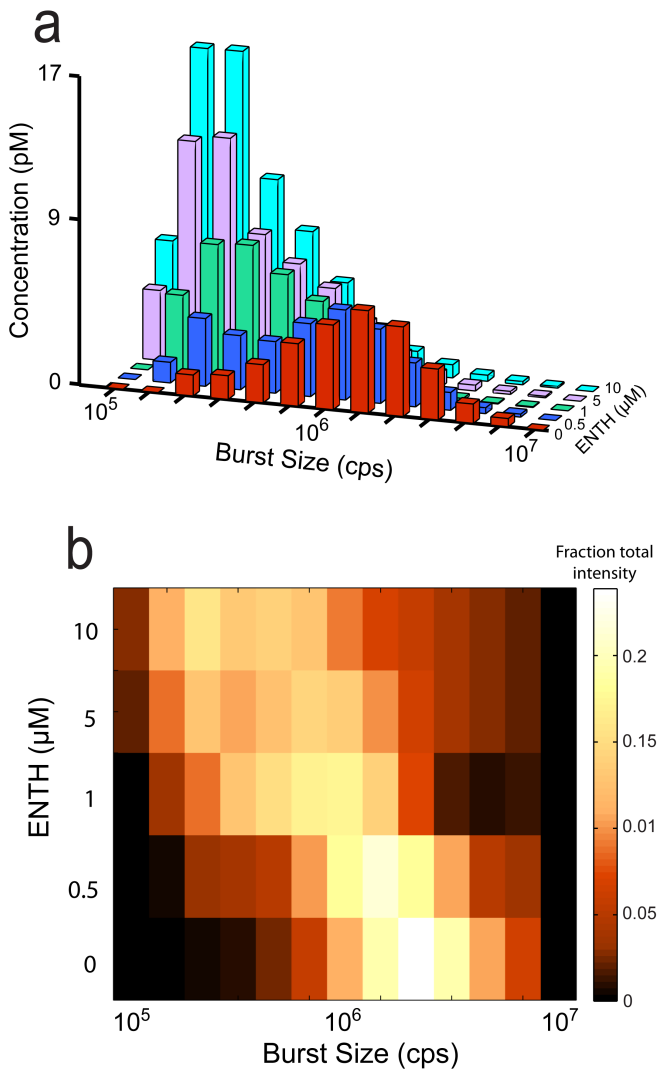

Figure 6. Dose dependence of ENTH-mediated vesiculation. (a) BAS histograms of 200 nm-diameter, TopFluor-labeled, (5%) PtdInsP(4,5)P2Folch liposomes before (red) and after incubation at 37 °C for 20 min with 500 nM (blue), 1 μM (green), 5μM (purple), and 10 μM (cyan) ENTH. (b) Heat-map representation of the fractional intensity for each reaction shown in (a). The data shown is representative of three experimental replicates.

nm diameter), the high protein concentration (10 μM), and the likelihood that the products, rather than vesicular in nature, are micellar [15].

The high sensitivity of BAS allowed us to address these concerns: (i) fission activity was observed at sub-micromolar protein concentration, (ii) fission activity does not depend on the curvature of starting liposomes, as those of 400 nm diameter worked as well as smaller ones and (iii) the products are consistent with 20 nm vesicles, as observed previously [14].

Furthermore, the high sensitivity of BAS allowed us to uncover attenuated membrane fission activity in experiments with the full-length epsin protein. Attenuation may suggest an inhibited conformation for full-length epsin, as has been suggested for syndapin, another protein involved in formation of vesicles at the recycling endosome [29]. Intermolecular interactions have also been observed to cause auto-inhibition, in the case of endophilin A1, a curvature-inducing endocytic protein that also contains an N-terminal amphipathic helix [30].

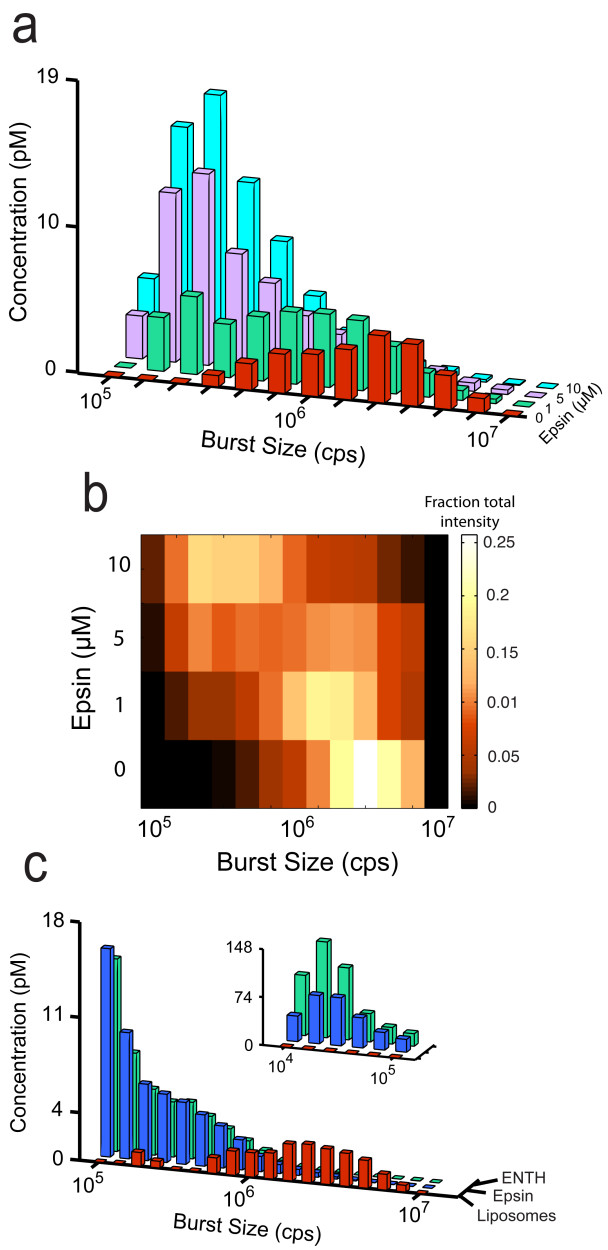

Figure 7. Full-length epsin has vesicle fission activity. (a)BAS histograms of 200 nm-diameter, TopFluor-labeled, (5%) PtdInsP(4,5)P2Folch liposomes before (red) and after incubation at 37 °C for 40 min with 1 μM (green), 5 μM (purple), and 10 μM (blue) full-length epsin. (b)Heat-map representation of the fractional intensity for each reaction **(Figure 7, Continued)** shown in (a). (c) Comparison of ENTH and epsin activity. BAS histograms of starting liposomes (red), and liposomes incubated at 37 °C for 90 min with 2 μM ENTH (blue) or full-length epsin (green). The data shown is representative of three experimental replicates.

CHAPTER III

SUMMARY AND FUTURE DIRECTIONS

Despite its central importance to the regulation of many cellular functions, the minimal machinery of vesicle fission remains a topic of debate. Integral protein machinery sometimes posses overlapping function as a sort of failsafe, complicating the interpretation of *in vivo* data. For example, related BAR domains may possess overlapping function with amphiphysin (AMPH-1) in *C. elegans*, convoluting interpretation of knockdown experiments [17]. This exemplifies the need for a simple *in vitro* assay for fission to ascribe clear roles to proteins in the fission. Here, we establish BAS as a highly sensitive, reagent sparing approach for the analysis of single particle dynamics of membrane fission reactions in free solution. Using BAS, we demonstrate that insertion of an amphipathic helix is sufficient to drive vesicle fission at physiologically relevant ENTH concentrations, as well as with full-length epsin.

Until recently, amphipathic helix insertion was proposed primarily as a means of inducing membrane curvature, similar to the insertion of cone-shaped lipids in one leaflet of the membrane. More recently, studies introduce an alternative role in which amphipathic helices act as fission catalysts. In contrast to the canonical model in which dynamin serves as the core fission machinery, our findings support a model in which insertion of these helices instigates fission instead. These findings are consistent with a number of pathways that involve fission independent of any dynamin-like protein. One such pathway is that of influenza viral budding, which relies on the amphipathic helix of

the ion channel M2 to induce fission [34]. Other examples include COPI and COPII coated vesicles which have been shown to use the amphipathic helices on Arf and Sar1, respectively [31;7]. In this study we lend support this hydrophobic insertion model for fission using a minimal system, demonstrating that insertion of an amphipathic helix is sufficient to drive vesicle fission even at physiologically relevant protein concentrations.

Using BAS, we demonstrate that both the ENTH domain and full-length epsin protein are sufficient for membrane fission. However, even at high protein concentration and 37 °C, the fastest reactions we observed proceeded on a timescale of minutes to tens of minutes. This suggests that other factors are required to increase the fission activity to physiologically significant rates, on the order of seconds to tens of seconds [32]. Notably, the results of recent studies indicated a reciprocal requirement for the amphipathic-helix containing amphiphysin and partner protein, dynamin, in order to stimulate membrane fission [15; 33]. Our results using BAS reopen the question of how membrane fission is induced, not only in endocytosis, but also, how transport carriers and vesicles are released at other locations in the cell, where dynamin does not appear to play a role. Our findings also raise others questions: how is epsin regulated, and what stimulates epsin-induced membrane fission? Finally, our findings indicate that BAS offers a highly sensitive approach to follow single particle dynamics of a membrane fission reactions in free-solution, for identification of membrane fission agents and characterization of the mechanism of membrane fission regulation.

Having established BAS as a viable assay for the investigation of membrane vesicle fission, we will utilize this technique in conjunction with a model protein system

in an effort to define the role of dynamin and dynamin-like proteins in this central process. To this end, our lab began collaboration with the Grant lab at Rutgers University, Department of Biochemistry. The Grant lab studies the endocytic recycling system in *C. elegans*. This system is simplified by the existence of only one dynamin-like protein, receptor mediated endocytosis protein-1, or RME-1. RME-1 is a dynamin structural homolog that is ubiquitously expressed in worm cells, eliminating any concern of neuron-specific activity [34]. Like dynamin, RME-1 also has the ability to tubulate acidic liposomes *in vitro*. RME-1 is believed to function in conjunction with its binding partner AMPH-1 to catalyze vesicle fission at the recycling endosome [17]. Lending support to a conserved mechanism of fission utilizing dynamin and dynamin-like proteins, AMPH-1 was initially implicated in endocytosis through its interaction with neuronal dynamin [35]. Our intention is to use this simplified system in conjunction with BAS to investigate the presumption that is RME-1 that acts as the core machinery, with the amphipathic helix-containing AMPH-1 playing a regulatory role in the fission reaction at the recycling endosome.

Consistent with our previous findings with both the ENTH domain and epsin, our preliminary results suggest that the amphipathic helix containing protein AMPH-1 is capable of inducing fission of phosphatidylserine (PS) liposomes (Figure 8). To our surprise, this activity is ATP dependent, suggesting a previously unobserved ATPase activity of AMPH-1. In stark opposition to the current dogma, our results suggest that RME-1 may play a regulatory role in the fission reaction, inhibiting AMPH-1 mediated fission (data not shown). It is worth noting that AMPH-1 mediated fission is

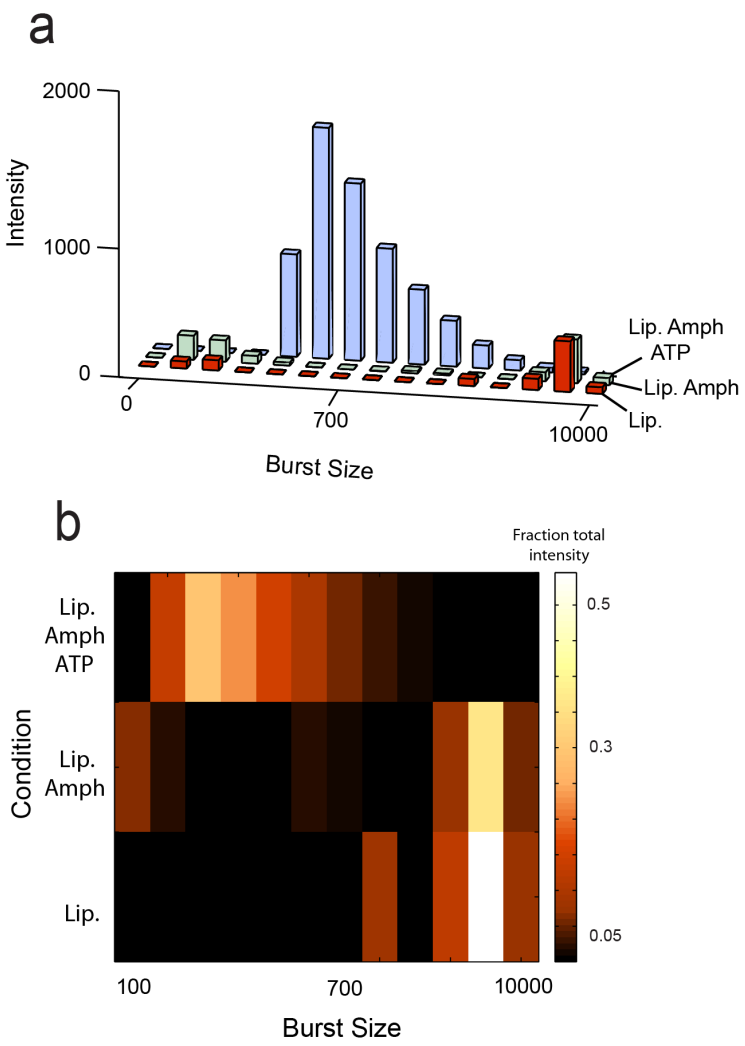

Figure 8. Amphiphysin has vesicle fission activity. (a) BAS histograms of 400 nm-diameter, Rhodamine labeled phosphatidylserine liposomes before (red) and after incubation at 21°C for 1 min with 10 μM amphiphysin (green), and 10 μM amphiphysin plus 2 mM ATP (blue). (b)Heat-map representation of the fractional intensity for each reaction shown in (a).

significantly attenuated compared to that of the ENTH domain. This is important for two reasons. First, this is indicative of the highly regulated fission activity that would be necessary to prevent aberrant fission in a cellular context. Second, it is unlikely that this activity would be decipherable using an alterative, less sensitive technique such as sedimentation. Taken together our findings suggest a conserved mechanism for fission in which amphipathic-helix containing proteins serve as the core machinery, with dynamin and dynamin-like proteins functioning as regulators. Future research will focus on characterizing the roles of the proteins in our minimal system using more physiologically relevant lipid composition, as well as characterizing the novel ATPase activity of AMPH-1 and its resultant effects on the modulation of fission. Taken together, our results present BAS as an extremely promising technique for the investigation of fission. By expanding our studies beyond RME-1 and AMPH-1, BAS will be instrumental in the identification of novel factors involved in this fundamental life process.

REFERENCES

1 Shpetner, H. S. & Vallee, R. B. Identification of dynamin, a novel mechanochemical enzyme that mediates interactions between microtubules. *Cell* **59**, 421-432 (1989).

2 Praefcke, G. J. & McMahon, H. T. The dynamin superfamily: universal membrane tubulation and fission molecules? *Nature Reviews. Molecular cell Biology* **5**, 133-147, doi:10.1038/nrm1313 (2004).

3 Sweitzer, S. M. & Hinshaw, J. E. Dynamin undergoes a GTP-dependent conformational change causing vesiculation. *Cell* **93**, 1021-1029 (1998).

4 Jakobsson, J. *et al.* Regulation of synaptic vesicle budding and dynamin function by an EHD ATPase. *The Journal of neuroscience : the official journal of the Society for Neuroscience* **31**, 13972-13980, doi:10.1523/JNEUROSCI.1289-11.2011 (2011).

5 Bashkirov, P. V. *et al.* GTPase cycle of dynamin is coupled to membrane squeeze and release, leading to spontaneous fission. *Cell* **135**, 1276-1286, doi:10.1016/j.cell.2008.11.028 (2008).

6 Liu, Y. W. *et al.* Differential curvature sensing and generating activities of dynamin isoforms provide opportunities for tissue-specific regulation. *Proceedings of the National Academy of Sciences of the United States of America* **108**, E234-242, doi:10.1073/pnas.1102710108 (2011).

7 Lee, M. C. *et al.* Sar1p N-terminal helix initiates membrane curvature and completes the fission of a COPII vesicle. *Cell* **122**, 605-617, doi:10.1016/j.cell.2005.07.025 (2005).

8 Hinshaw, J. E. & Schmid, S. L. Dynamin self-assembles into rings suggesting a mechanism for coated vesicle budding. *Nature* **374**, 190-192, doi:10.1038/374190a0 (1995).

9 Kozlovsky, Y. & Kozlov, M. M. Membrane fission: model for intermediate structures. *Biophysical journal* **85**, 85-96, doi:10.1016/S0006-3495(03)74457-9 (2003).

10 Danino, D., Moon, K. H. & Hinshaw, J. E. Rapid constriction of lipid bilayers by the mechanochemical enzyme dynamin. *Journal of structural biology* **147**, 259-267, doi:10.1016/j.jsb.2004.04.005 (2004).

11 Shupliakov, O. *et al.* Synaptic vesicle endocytosis impaired by disruption of dynamin-SH3 domain interactions. *Science* **276**, 259-263 (1997).

12 Chen, H. *et al.* Epsin is an EH-domain-binding protein implicated in clathrin-mediated endocytosis. *Nature* **394**, 793-797, doi:10.1038/29555 (1998).

13 McMahon, H. T. & Gallop, J. L. Membrane curvature and mechanisms of dynamic cell membrane remodelling. *Nature* **438**, 590-596, doi:10.1038/nature04396 (2005).

14 Boucrot, E. *et al.* Membrane fission is promoted by insertion of amphipathic helices and is restricted by crescent BAR domains. *Cell* **149**, 124-136, doi:10.1016/j.cell.2012.01.047 (2012).

15 Neumann, S. & Schmid, S. L. Dual role of BAR domain-containing proteins in regulating vesicle release catalyzed by the GTPase, dynamin-2. *The Journal of biological chemistry* **288**, 25119-25128, doi:10.1074/jbc.M113.490474 (2013).

16 Haucke, V. Membrane biology: fission behind BARs. *Current biology : CB* **22**, R455-457, doi:10.1016/j.cub.2012.04.035 (2012).

17 Pant, S. *et al.* AMPH-1/Amphiphysin/Bin1 functions with RME-1/Ehd1 in endocytic recycling. *Nature cell biology* **11**, 1399-1410, doi:10.1038/ncb1986 (2009).

18 Chizmadzhev, Y. A. *et al.* Lipid flow through fusion pores connecting membranes of different tensions. *Biophysical journal* **76**, 2951-2965, doi:10.1016/S0006-3495(99)77450-3 (1999).

19 Wickner, W. & Schekman, R. Membrane fusion. *Nature structural & molecular biology* **15**, 658-664 (2008).

20 Roux, A. Reaching a consensus on the mechanism of dynamin? *F1000prime reports* **6**, 86, doi:10.12703/P6-86 (2014).

21 Pucadyil, T. J. & Schmid, S. L. Real-time visualization of dynamin-catalyzed membrane fission and vesicle release. *Cell* **135**, 1263-1275, doi:10.1016/j.cell.2008.11.020 (2008).

22 Neumann, S., Pucadyil, T. J. & Schmid, S. L. Analyzing membrane remodeling and fission using supported bilayers with excess membrane reservoir. *Nature protocols* **8**, 213-222, doi:10.1038/nprot.2012.152 (2013).

23 Wang, L. H., Sudhof, T. C. & Anderson, R. G. The appendage domain of alpha-adaptin is a high affinity binding site for dynamin. *The Journal of biological chemistry* **270**, 10079-10083 (1995).

24 Legendre-Guillemin, V., Wasiak, S., Hussain, N. K., Angers, A. & McPherson, P. S. ENTH/ANTH proteins and clathrin-mediated membrane budding. *Journal of cell science* **117**, 9-18, doi:10.1242/jcs.00928 (2004).

25 Simpson, F. *et al.* SH3-domain-containing proteins function at distinct steps in clathrin-coated vesicle formation. *Nature cell biology* **1**, 119-124, doi:10.1038/10091 (1999).

26 Ford, M. G. *et al.* Curvature of clathrin-coated pits driven by epsin. *Nature* **419**, 361-366, doi:10.1038/nature01020 (2002).

27 Puchalla, J., Krantz, K., Austin, R. & Rye, H. Burst analysis spectroscopy: a versatile single-particle approach for studying distributions of protein aggregates and fluorescent assemblies. *Proceedings of the National Academy of Sciences of the United States of America* **105**, 14400-14405, doi:10.1073/pnas.0805969105 (2008).

28 Krantz, K. C. *et al.* Clathrin coat disassembly by the yeast Hsc70/Ssa1p and auxilin/Swa2p proteins observed by single-particle burst analysis spectroscopy. *The Journal of biological chemistry* **288**, 26721-26730, doi:10.1074/jbc.M113.491753 (2013).

29 Rao, Y. *et al.* Molecular basis for SH3 domain regulation of F-BAR-mediated membrane deformation. *Proceedings of the National Academy of Sciences of the United States of America* **107**, 8213-8218, doi:10.1073/pnas.1003478107 (2010).

30 Chen, Z. *et al.* Intradimer/Intermolecular interactions suggest autoinhibition mechanism in endophilin A1. *Journal of the American Chemical Society* **136**, 4557-4564, doi:10.1021/ja411607b (2014).

31 Beck, R. *et al.* Coatomer and dimeric ADP ribosylation factor 1 promote distinct steps in membrane scission. *The Journal of cell biology* **194**, 765-777, doi:10.1083/jcb.201011027 (2011).

32 Taylor, M. J., Perrais, D. & Merrifield, C. J. A high precision survey of the molecular dynamics of mammalian clathrin-mediated endocytosis. *PLoS biology* **9**, e1000604, doi:10.1371/journal.pbio.1000604 (2011).

33 Meinecke, M. *et al.* Cooperative recruitment of dynamin and BIN/amphiphysin/Rvs (BAR) domain-containing proteins leads to GTP-dependent membrane scission. *The Journal of biological chemistry* **288**, 6651-6661, doi:10.1074/jbc.M112.444869 (2013).

34 Grant, B. *et al.* Evidence that RME-1, a conserved C. elegans EH-domain protein, functions in endocytic recycling. *Nature cell biology* **3**, 573-579, doi:10.1038/35078549 (2001).

35 David, C., McPherson, P. S., Mundigl, O. & de Camilli, P. A role of amphiphysin in synaptic vesicle endocytosis suggested by its binding to dynamin

in nerve terminals. *Proceedings of the National Academy of Sciences of the United States of America* **93**, 331-335 (1996).

36 Brooks, A., Shoup, D. Kustigian, L., Puchalla, J., Carr, C. M., & Rye, H. S. Single Particle Fluorescenec Burst Analysis of Espin Induced Membrane Fission. *PLoS ONE* **10**, e0119563, doi:10.1371/jounal.pone.0119563 (2015).